# a METHOD of RADOME COMPENSATION BROADBAND

Many radar systems require an antenna cover for protection from environmental conditions. Stationary land-based radar antennas are usually protected from such weather conditions as ice and snow by a hemispherical dome that encloses the radar antenna. Supersonic aircraft require streamlined covers over their scanning radar antennas for both environmental protection and aerodynamic stability. In any radar application the radome must provide a certain level of electrical performance in addition to satisfying certain mechanical and physical requirements. In most situations the electrical engineer must work with a radome material and shape that have been specified from environmental and aircraft stability requirements. The goal of the electrical design is development of a radome that provides low attenuation of the radar signal, with very small change in the apparent angle-of-arrival.

The Applied Physics Laboratory has conducted research and development in supersonic, streamlined, ceramic radomes for missile and general application since 1954. Initial efforts were directed toward development of a material that would withstand rain erosion; resulting from this effort, a new ceramic-like material, Pyroceram,* developed by Corning Glass Works Inc., was introduced for radome application.

Radome evaluation and boresight-correction studies at APL have demonstrated that a radome with a tapered wall thickness can be designed to have low boresight errors and high transmission. Simple electrical designs that have produced low boresight error ($< 0.2$ spatial degree) and high transmission ($> 80\%$) over a 3 to 4% frequency band will be discussed.

The use of a simplified radome mathematical model provides for a quick and easy initial design, but this usually requires modification by empirical laboratory techniques. It is significant, however, that regardless of the modifications required, a tapering technique does exist for developing a radome with low boresight error.

It is reasonable to assume that a radome and antenna would be designed as a single integrated unit. In many applications, however, development of the antenna precedes that of the radome. Such is the case with the radome application to be de-

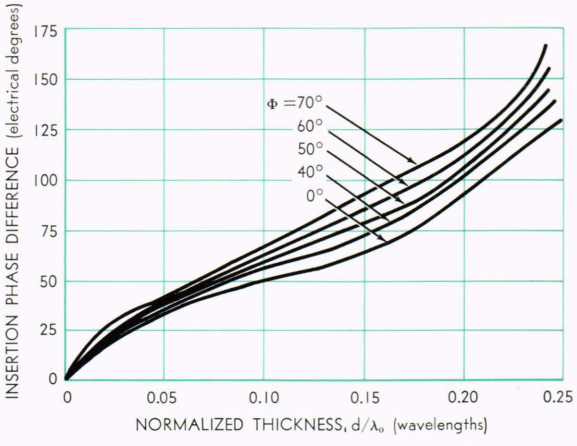


**Fig. 1—Insertion phase difference versus $d/\lambda_0$, thickness in wavelengths for circular polarization or 45° incidence linear polarization. The dielectric constant is 5.5.**

* See also "Radome Thermal Design for a Mach 4 Missile," by R. P. Suess and L. B. Weckesser, *APL Technical Digest*, 3, July–Aug. 1964, 13–17.

# with CAPABILITY

*Boresight-error measurements on tapered solid-wall radomes have provided an experimental boresight bandwidth of 3.6%. Boresight bandwidth is defined as the frequency band over which boresight-error slopes are less than 0.01 degree/degree in any 20° gimbal rotation. Theoretical bandwidths extrapolated from experimental data indicate that bandwidths as high as 5% are obtainable with ceramic radomes having a relative dielectric constant of 5.5.*

R. H. Hallendorff

scribed. Two different antennas of a phase interferometer system were used for boresight measurements of corrected radomes. One is a circularly polarized, four-quadrant (two interferometers located in orthogonal gimbal planes) end-fire array. The other is a four-quadrant, linearly polarized, slotted waveguide array with the polarization vector at 45° to the gimbal planes. Both interferometer antennas have similar electrical phase center separations. The initial radome design and corrections were associated with the circularly polarized antenna because of its improved electrical symmetry.

The goal of this effort was development of a radome for either or both antennas with boresight and crosstalk error slopes less than 0.01 degree/degree over a 20° gimbal rotation and transmission losses less than 1 db over a 9% bandwidth using a ceramic radome that has a relative dielectric constant ($\epsilon_r$) of 5.5.

The objective of the tapered-wall investigations was to devise a taper that would reduce the angular error to zero at a single design frequency. The resulting boresight bandwidth (i.e., frequency band where the angular error slope is less than 0.01 spatial degree/degree within any 20° gimbal rotation) could then be determined experimentally. Only a 3 to 4% bandwidth was experimentally demonstrated. However, the achievement of even a 3 to 4% bandwidth is a significant improvement over previous measured radomes and thus establishes an improved standard for future radome broadbanding studies.

The experimental method used to construct a radome taper is to start with a thin radome and coat it to the appropriate thickness with a machinable compound whose electrical properties match those of the radome material. After a basic thickness has been built up, the radome taper can then be turned continuously or in steps on a contour-follower lathe.

## Theoretical Discussion

Two basic design approaches are presented for discussion. Both are developed to show that simple, graphical and mathematical procedures are available for quick and easy application to radome design. The first was used for actual construction of initial radome tapers. The second is presented to show that improved and simple prediction methods are available for deriving boresight-correcting tapers. In both cases antenna parameters such as aperture area, beamwidth, and near-field distortions are neglected. A complete radome analysis that includes antenna characteristics as well as

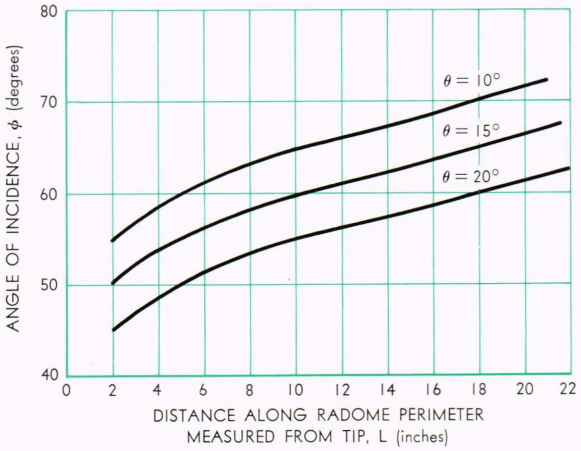


**Fig. 2—Incident angle versus distance along the radome perimeter.**

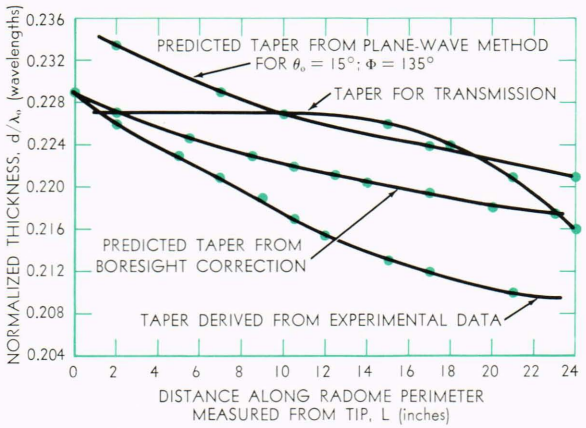


**Fig. 3—Comparison of theoretical and experimental tapers, $d/\lambda_0$ versus $L$.**

radome effects is a three-dimensional problem that requires the use of a computer. The experimental accuracy of the following approaches may suggest improved computer methods for radome analysis.

The first basic concept used in deriving a radome taper is to alter the radome-wall thickness in such a way that the insertion phase at one gimbal angle, defined as the critical gimbal angle $\theta_o$, remains constant along the radome contour. Measurements on constant-wall radomes have shown that a boresight-error maximum occurs consistently around certain gimbal angles, typically 10 to 20°, depending on radome aspect ratios, etc. The approach of initial tapering was to reduce the error at the critical gimbal angle without disturbing the error in the crosstalk plane or at other gimbal angles. Since crosstalk errors are related to radome-antenna symmetry, an axially symmetrical longitudinal taper should not affect the crosstalk error.

Plane-wave energy incident at the critical gimbal angle must retain its plane-wave phase characteristic upon passing through the radome wall. (It is assumed that refraction and reflection occur only in the boresight plane of the system; this assumption reduces the complex three-dimensional problem to a simple two-dimensional one. Absorption loss is also neglected.) The variation of insertion-phase difference $\Phi_o$† for circular or 45° linear polarization as a function of dielectric thickness is determined from equal superposition of perpendicular and parallel polarizations. A typical insertion-phase difference for flat-plate dielectrics for linear polarizations is given by

$$\Phi_o = \frac{2\pi d}{\lambda_o}\left(\sqrt{\epsilon_r - \sin^2\phi} - \cos\phi\right) + \arctan\frac{R^2_{12}\sin 2a}{1 - R^2_{12}\cos 2a},$$

where $a$ is $\frac{2\pi d}{\lambda_o}\left(\sqrt{\epsilon_r - \sin^2\phi}\right)$, $\phi$ is the angle of incidence, $\epsilon_r$ is the relative dielectric constant, $R_{12}$ is the reflection coefficient from air to the dielectric medium, $\lambda_o$ is the free-space design wavelength, and $d$ is the thickness of the plate. (Two-dimensional flat-plate theory is assumed adequate for application to curved radome surfaces.)

A plot of insertion-phase differences derived for circular or 45° linear polarization is shown in Fig 1. As the incident angle $\phi$ is varied, a corresponding variation in $d/\lambda_o$ is required to maintain constant phase difference. The variation of incident angle along the radome perimeter $L$ is shown in Fig. 2 for various gimbal angles. The data from Figs. 1 and 2 are used to determine the required taper, i.e., the variation of $d/\lambda_0$ as a function of $L$ along the radome perimeter. Theoretically, correction is needed only along that portion of the radome contour illuminated by the receiver antenna; however, since the total radome curvature is illuminated by incoming R-F, a correction taper is made over the total length to assure compensation. A typical taper derived for $\Phi = 135°$ and $\theta = 15°$ is shown in Fig. 3. Note that no mention has been made of transmission requirements. The final design is completed by experimentally varying the taper about the design value.

A second analysis that predicts similar corrections is more descriptive of the actual physical system and determines thickness variations for both boresight and transmission requirements. It incorporates the simple graphical and mathematical procedures

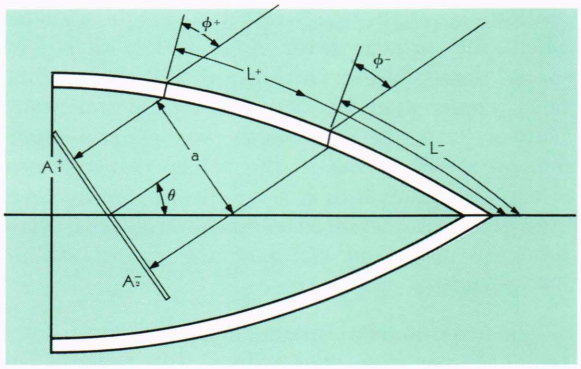


**Fig. 4—Monopulse system with phase interferometer and radome.**

† Insertion phase difference (I.P.D.) is defined as the difference between the phase in the dielectric medium and in air.

of optical ray tracing. Figure 4 shows a typical configuration of phase interferometer and radome. (It is assumed that each antenna responds only to energy propagated along a single optical path.) Antenna $A_1$ is designated as the leading positive aperture and $A_2$ as the lagging negative aperture for a given gimbal direction. A physical separation $a$ defines the interferometer gain of the antenna pair. Graphical methods were used to determine the angle of incidence as a function of station position along the perimeter as the antenna system is rotated. Figure 5 is a plot of the angle of incidence versus perimeter location $L$ for both $A_1^+$ and $A_2^-$. Note that at each gimbal angle (except 0°) the antenna apertures look through the radome at different points along the perimeters with different angles of incidence. This characteristic contributes to the boresight error.

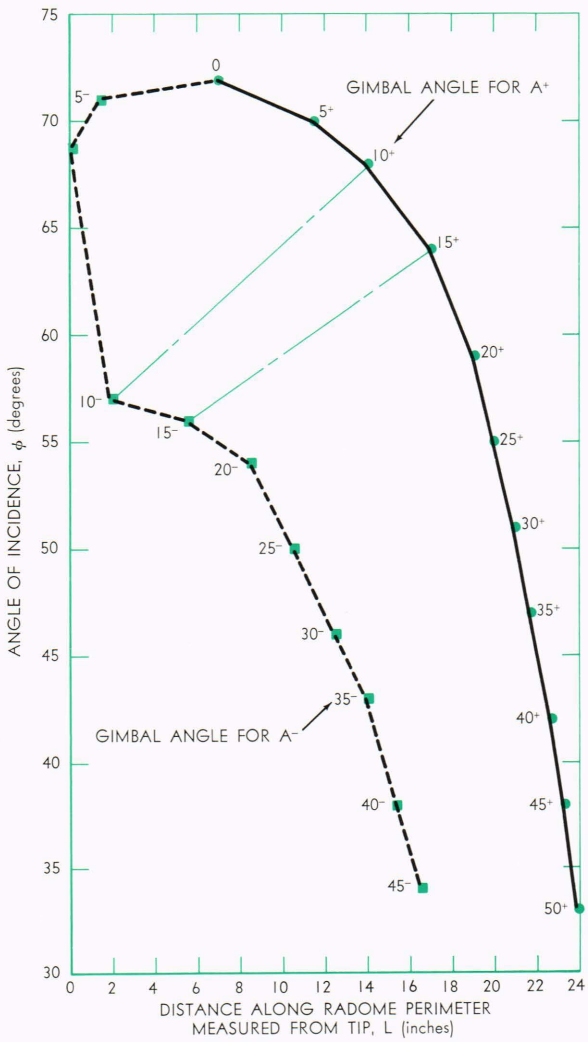


**Fig. 5—Incident angle variation ($\phi$) along radome perimeter $L$ for apertures $A^+$ and $A^-$.**

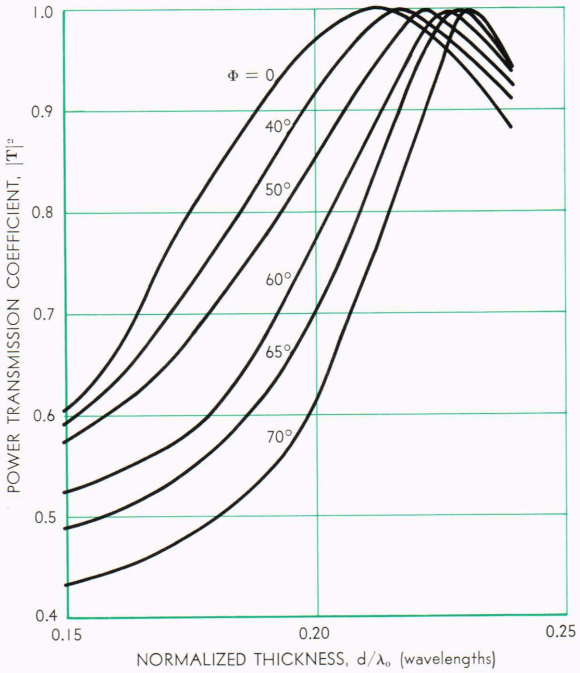


**Fig. 6—Power transmission $|T|^2$ versus $d/\lambda_0$ thickness for various incident angles.**

Optimum transmission for large incident-angle variations is required to preserve the amplitude distribution across the antenna aperture when no dome is present. A change in aperture amplitude distribution will result in a change of antenna performance. The amount of change for a given radome transmission characteristic is, however, not easily analyzed. Some positions along the radome perimeter must pass waves over wide ranges of angles of incidence. For example, from Fig. 5 at $L = 2$ in., the incident angle ranges from 71° to 57°. At $L = 12$ in., the variation is from 47° to 70°. To determine the best thickness for a range of incident angles, a plot of power transmission coefficient $|T|^2$ versus $d/\lambda_0$ is plotted in Fig. 6. Note that when $d/\lambda_0 = 0.277$, 97% transmission is obtained for all incident angles between 0° and 70°. This thickness is thus optimum for regions along the radome perimeter where large ranges of incident angles must be compensated for maximum transmission. Using data from Figs. 5 and 6, thickness variations are derived for optimum transmission through the radome for all gimbal angles (see Fig. 3). The boresight correction taper is then matched as closely as possible to the taper derived for optimum transmission.

For boresight-error correction, a change in thickness is required to compensate for the phase difference between signals received at each aperture

TABLE I

BORESIGHT CORRECTION DATA

| *Gimbal Angle* ($\theta$) | *Region of Correction* ($L^-$ *to* $L^+$) (*inches*) | *Range of Angle of Incidence* (*degrees*) | *Required Thickness Correction* (*wavelength*) | *Rate of Correction* (*wavelength/in.*) |
|---|---|---|---|---|
| 10 | 2.0 to 14.0 | 57 — 68 | 0.0080 | 0.000656 |
| 15 | 5.5 to 17.0 | 56 — 64 | 0.0053 | 0.000460 |
| 20 | 8.5 to 19.0 | 54 — 59 | 0.0033 | 0.000314 |
| 25 | 10.5 to 20.0 | 50 — 54 | 0.0025 | 0.000264 |
| 30 | 12.5 to 21.0 | 46 — 51 | 0.0032 | 0.000376 |
| 35 | 14.0 to 21.5 | 43 — 47 | 0.0024 | 0.000321 |
| 40 | 15.0 to 22.5 | 38 — 42 | 0.0022 | 0.000293 |
| 45 | 16.5 to 23.5 | 34 — 38 | 0.0020 | 0.000286 |

since each aperture receives energy at different angles of incidence. For boresight-error correction at $\theta = 10°$, the thickness that $A^+$ ($\phi = 68°$) looks through must be less than that of $A^-$ ($\phi = 57°$) in order to obtain zero phase difference between the received signals. From Fig. 5 it is shown that at $\theta = 10°$, the thickness correction must be applied over a region along the radome perimeter from $L = 2$ in. to $L = 14$ in. The magnitude of the change is found from Fig. 7 for incident-angle variation between $\phi_+ = 68°$ and $\phi_- = 57°$ as $\Delta(d/\lambda_0) = -0.0315 - (-0.0235) = -0.0080$ wavelength. Table I presents the amount of thickness correction required over a region of radome perimeter for gimbal angles between 10° and 45°.

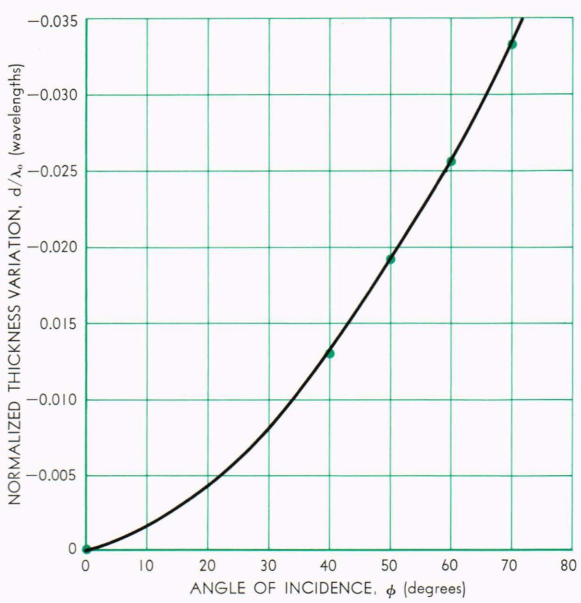


**Fig. 7—Normalized thickness variation for a constant insertion phase difference versus incident angle averaged over $0.200 \leq d/\lambda_0 \leq 0.240$.**

(Gimbal angles of 0° and 5° have been neglected since each aperture at these gimbal angles receives almost identical signal phase.) Note that many regions of boresight correction overlap one another. For example, at $\theta = 10°$, a correction rate of $0.656 \times 10^{-3}$ wavelength/in. is needed over a region from $L = 2$ in. to $L = 14$ in., while for $\theta = 15°$, a correction rate of $0.46 \times 10^{-3}$ is needed over a region from $L = 5.5$ in. to $L = 17$ in. The two regions overlap from $L = 5.5$ in. to $L = 14$ in. To determine an overall correction, the rates $\Delta(d/\lambda_0)/\Delta L$ are averaged over the radome perimeter. This is a relative thickness variation and can be matched to the thickness variation derived for optimum transmission. Boresight and transmission tapers are matched along the high incidence-angle regions of the radome perimeter since these are the most critical to correct. The boresight taper was matched to the amplitude taper at $L = 2$ in. A comparison is made of this taper design for boresight correction and that derived from experimental data in Fig. 3. Agreement between theoretical and experimental tapers are within 0.002 wavelength at the critical high incidence-angle regions and within 0.008 wavelength overall.

## Experimental Tests

All laboratory tapers were designed from theory generated by plane-wave correction at a critical gimbal angle. Various tapers of different basic thicknesses with similar taper rates were constructed and evaluated. The first successful taper (taper No. 1) varied between $d_{\min}/\lambda_o = 0.217$ and $d_{\max}/\lambda_o = 0.236$. Figure 8 shows that a minimum boresight error of 0.13 spatial degree occurs at approximately $f/f_o = 0.973$, where $f_o$ is design frequency associated with design wavelength, with a resultant boresight bandwidth of about 2.8%. Figure 9 shows a plot of typical boresight-error curves

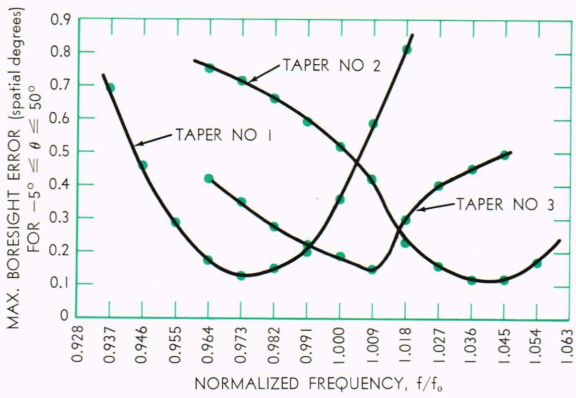


**Fig. 8—Maximum boresight error over frequency band for three different experimental tapered domes.**

over a 9% bandwidth for a tapered radome. A second taper was constructed by uniformly reducing the thickness of the No. 1 taper to optimize the radome for a higher frequency. Figure 8 shows that minimum error occurred around $f/f_o = 1.04$. The boresight bandwidth of taper No. 2 is around 3.6%. A third taper with a mean thickness between tapers No. 1 and 2 was constructed for optimizing near $f/f_o = 1.0045$. Minimum boresight was obtained near $f/f_o = 1.009$, but bandwidth was reduced to about 1.8%. No effort was made to reduce the bandwidth degredation of taper No. 3. Boresight-error curves over a 9% frequency band for both a circularly and a linearly polarized antenna, using the No. 3 tapered radome, are very similar; however, the crosstalk errors for the two antennas are quite different (Fig. 10). It is probable that this difference is related to antenna symmetry.

Relative transmission losses for circular polarization in both the boresight and crosstalk planes are shown in Fig. 11 over a 9% bandwidth, using the taper No. 3 radome. It is noted that maximum transmission efficiency occurs around $f/f_o = 1.045$, while minimum boresight error, as shown in Fig. 8, occurs near $f/f_o = 1.009$. It is reasonable to expect that high transmission and low boresight features should coincide at the same frequency. These experimental conditions indicate, therefore, that the tapers used are not necessarily the optimum available for simultaneous transmission and boresight correction.

## Illumination Depolarization

Boresight errors of constant-wall radomes have shown a dependence on depolarization. This is defined as the difference between illuminating polarization and receiver antenna polarization. A number of experiments were conducted to determine the effect of depolarization on a corrected radome for both a circularly and a linearly polarized system. Elliptically polarized illuminations were transmitted through the radome with different magnitudes of ellipticity and different major axis orientations. Ellipticity was defined as the log ratio of power along the major axis to that along the minor axis. It was determined that a 3- to 4-db

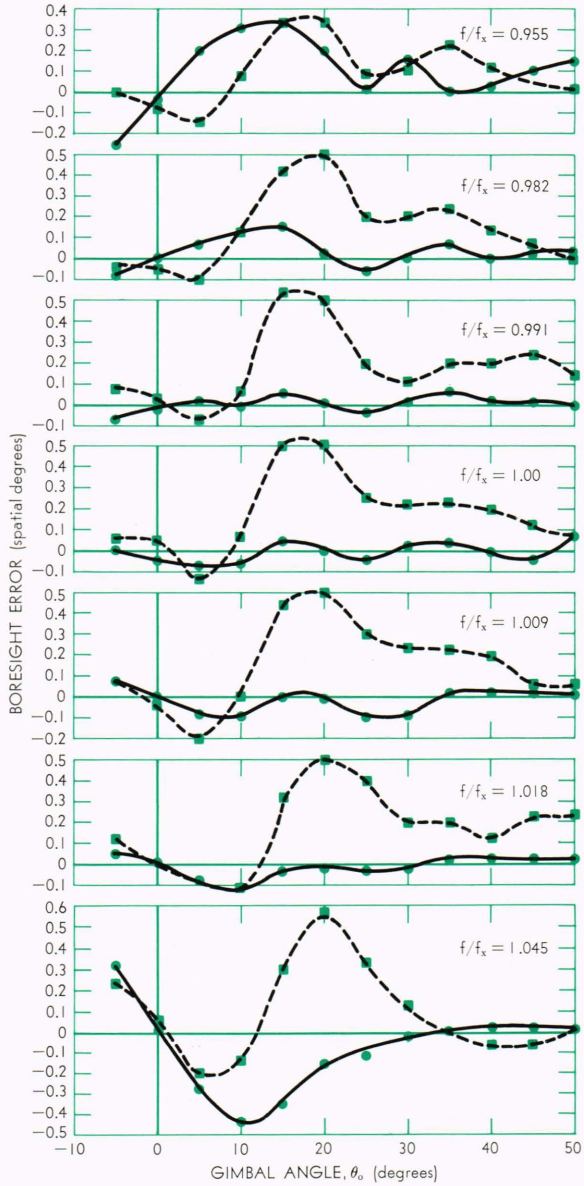


**Fig. 9—Boresight error for No. 1 tapered radome, $f_x = 0.973\ f_o$, where $f_x$ is the frequency at which minimum boresight error occurs. For comparison, the boresight error of the untapered radome is shown in broken line.**

ellipticity could be tolerated for all major axis orientations before bandwidth degradation occurred. The linear depolarization study showed similar bandwidth degradation when the illuminating polarization was changed with respect to the receiving antenna. Experimental boresight-error data show that boresight errors are dependent upon the incident polarization, and that a given taper is satisfactory only for a limited range of polarization;[1] however, tapered-wall radomes provide an average overall depolarization effect that is much less than in constant-wall-radomes that we have investigated in the past.

## Conclusions

Experimental results show that a satisfactory low boresight (0.01 degree/degree) system using a streamlined tapered-wall ceramic radome can be developed for operation over at least a 3% boresight bandwidth. Extrapolation of experimental data indicates that theoretical boresight bandwidths up to 5 to 6% are achievable with tapered-wall radomes having an $\epsilon_r$ of about 5.5.

Experimental and predicted radome designs indicate that boresight correction of a phase monopulse radome is characterized by a longitudinal decreasing wall thickness from tip to base for radome thicknesses near a half wave. Simplification of the design procedure can provide quick and easy calculations for absolute thicknesses and taper rates with better than "ball-park" accuracies. However, experimental differences between transmission and boresight features of experimental, tapered-wall radomes indicate that additions to the design procedure are needed for improved radome correction designs.

Crosstalk error differences between a linearly polarized and circularly polarized antenna array are quite large, indicating a need for further antenna evaluation. Correction of a radome for all polarizations remains a difficult problem to solve; however, tapered-wall radomes do provide an overall average improvement over previous radomes.

The reasonably successful calculations of boresight correction designs from relatively simple concepts have resulted in the development of an improved radome analysis using computer techniques. Future computer programs can now be tested and verified by correlating the experimental solutions uncovered and discussed in this report.

[1] R. E. Webster and D. P. Moore, "Elliptical Polarizations and Radome Wall Design," *Proceedings of the OSU-WODC Radome Symposium*, I, June 1957, p. 14.

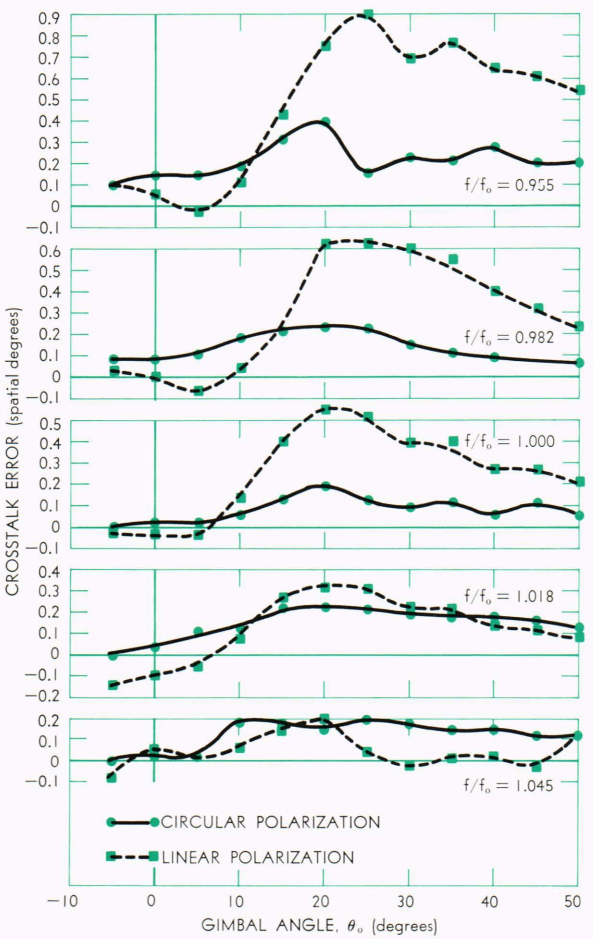


**Fig. 10—Crosstalk errors for a circularly and linearly polarized antenna system with a tapered No. 3 radome.**

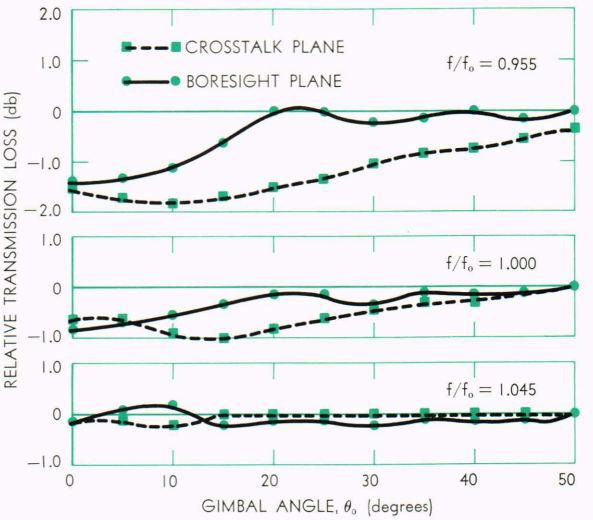


**Fig. 11—Transmission loss for a tapered No. 3 radome.**